Antimatter-wave interferometry in QUPLAS

Simone Sala, for the QUPLAS collaboration †
Dipartimento di Fisica, Università degli Studi di Milano, I-20133 Milano, Italy
and INFN Sezione di Milano, I-20133 Milano, Italy

UNIVERSITÀ DEGLI STUDI DI MILANO
DIPARTIMENTO DI FISICA

The QUPLAS project and its goals

QUantum interferometry and gravity with **P**ositrons and **LAS**ers, a staged experiment in antimatter interferometry:

- **QUPLAS-0**: Talbot-Lau interferometry with $10-18\,\mathrm{keV}$ **positrons** (e^+) and **electrons** (e^-) (1).
- **QUPLAS-I**: Matter wave interferometry on ortho-**positronium** (ortho-Ps), an unstable ($\tau = 142\,\mathrm{ns}$) bound state of e^+/e^-.
- **QUPLAS-II**: Weak equivalence principle tests on Ps: **measurement of** g_{Ps} with Talbot-Lau inertial sensing (2).

The QUPLAS collaboration †

S. Aghion, A. Ariga, T. Ariga, M. Bollani, F. Castelli, S. Cialdi, K. Edler, A. Ereditato, C. Evans, R. Ferragut, M. Giammarchi, M. Leone, M. Longhi, G. Maero, S. Olivares, C. Pistillo, M. Potenza, M. Romé, S. Sala, P. Scampoli.

Theory

The core of QUPLAS: a **Talbot-Lau two-grating interferometer**, with unequal distances $(L, \eta L)$ and grating periods (d_1, d_2). The **Talbot length** $L_T = \frac{d_2^2}{\lambda}$ is the typical length scale, $\lambda = h/p_y$ being the de Broglie wavelength.

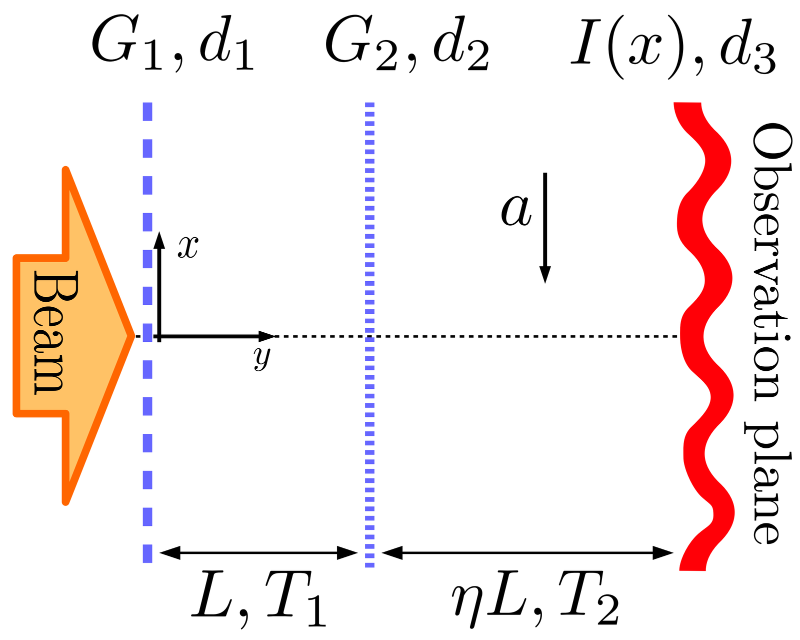

Figure 1: Asymmetric Talbot-Lau setup. An external uniform acceleration a acts on the particles. $T_{1,2}$ are the times of flight, assuming rectilinear motion along y.

Under the resonance conditions $\eta = \frac{1}{d_1/d_2 - 1}$ and $L = \frac{d_1}{d_2} L_T$, high contrast fringes appear, with a **magnified period** (2):

$$d_3 = \eta d_1.$$

The external force produces a measurable rigid displacement of the interference fringes:

$$\Delta x = a\frac{T_1^2}{2}\eta(\eta+1),$$

The **inertial sensitivity**, σ_a/a (relative error on the measured acceleration), depends on the fringe visibility, the integrated flux, N_0, and the longitudinal velocity distribution.

Considering all this factors **Asymmetric configurations can be more effective** for inertial sensing (2). This is relevant for the QUPLAS-II phase.

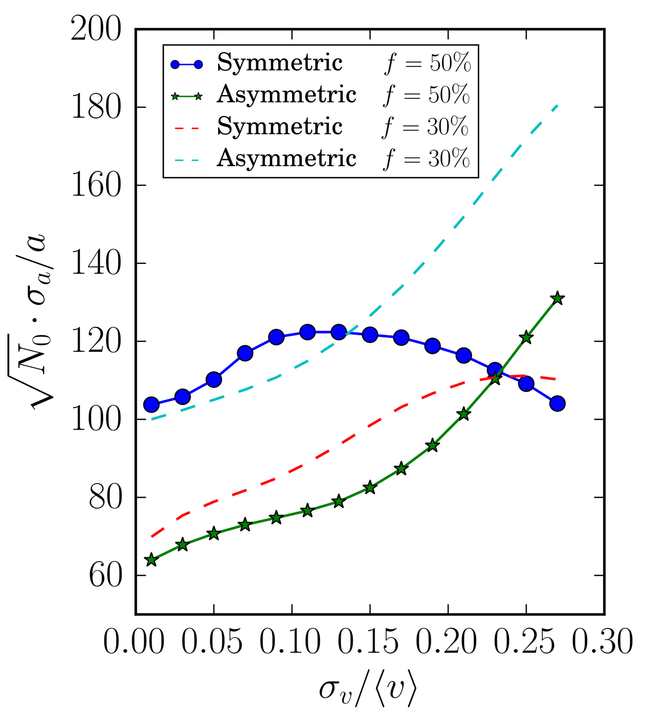

Figure 2: Inertial sensitivity vs width of the (Gaussian) particle speed distribution; f is the open fraction of the gratings and the asymmetric $\eta = 2$ (see Fig.1) configuration is compared against the standard setup ($\eta = 1$, $d_1 = d_2$). A total length $L = 1\,\mathrm{m}$ and $\langle v\rangle = 800\,\mathrm{ms}^{-1}$ are assumed.

The diffraction gratings

The Silicon Nitride (SiN) diffraction gratings have been manufactured to our specifications by LumArray, Inc. (a spinoff comopany of the NanoStructures laboratory at MIT) using interferometric litography techniques (5).

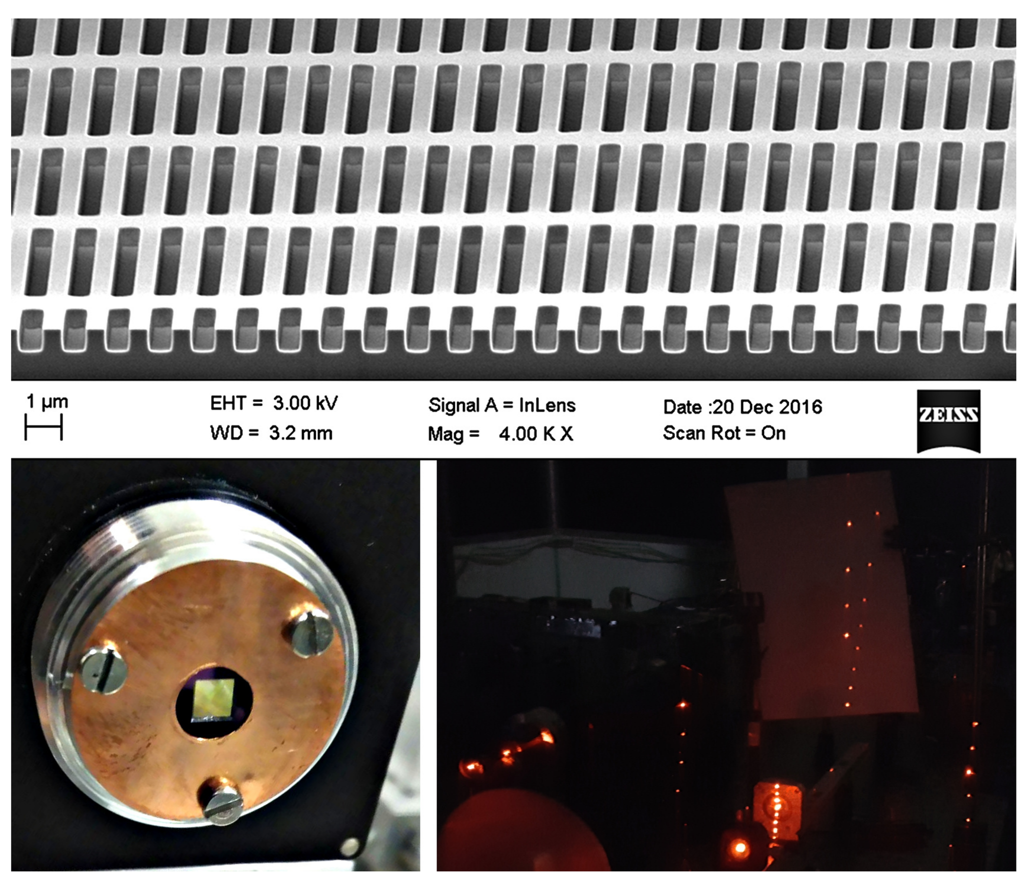

Figure 3: Top: SEM image of the free standing $600\,\mathrm{nm}$ thick SiN membrane. The $d = 1.2\,\mu\mathrm{m}$ slits run horizontally, with a $7\,\mu\mathrm{m}$ periodic support structure in the orthogonal direction. **Bottom left:** The $3 \times 3\mathrm{mm}^2$ wide membrane is clearly visible on a mounted grating. **Bottom right:** at optical wavelengths, far field diffraction can be exploited for rotational alignment.

Application: the QUPLAS-0 interferometer

Positron interferometry will be carried out using a **continuous** e^+ **beam** housed at the **L-NESS laboratory in Como** (3). Positrons produced by a ^{22}Na radioactive source are moderated by a monocrystalline tungsten film and electrostatically guided, with a **tunable energy** up to $18\,\mathrm{keV}$.

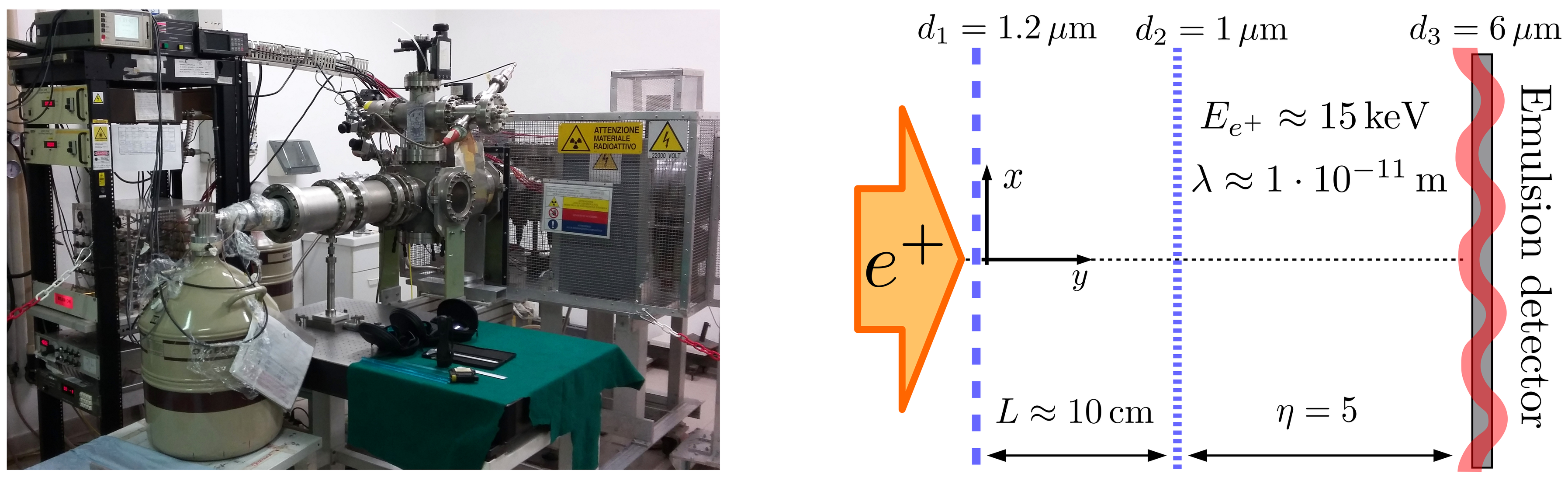

Figure 4: Left: picture of the positron beam facility (3); the final section of the vacuum chamber houses the QUPLAS-0 interferometer. **Right:** scheme of the $\eta = 5$ magnifying Talbot-Lau setup chosen as the optimal configuration for QUPLAS-0.

QUPLAS-0 will exploit **nuclear emulsions** as a position sensitive detector for the micrometric fringes. A new emulsion based detector was developed and tested for this purpose (4):

- **Gel enriched in silver bromide crystals** ($\sim 55\%$ vol.), on **glass substrate** for increased stability.
- Samples **exposed to the L-NESS beam** at various energies, e^+ intensity monitored by two HPGe detectors sensitive to the $511\,\mathrm{keV}$ gamma signal from annihilation.
- Emulsions analysed at the **automatic microscope scanning facility** of the University of Bern.
- **Detection efficiency** estimated comparing the expected and detected e^+ count.

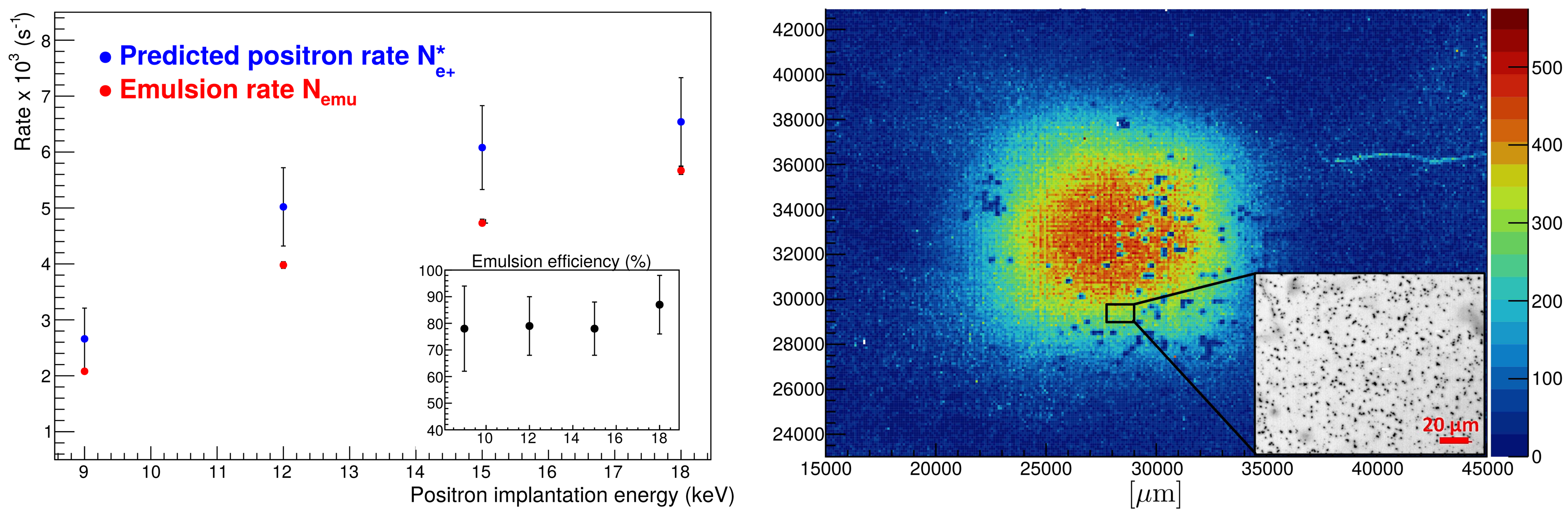

Figure 5: Left: Experimental results of a test exposure of emulsion films to the bare e^+ beam (4). Positrons below $9\,\mathrm{keV}$ annihilate within the $\approx 1\,\mu\mathrm{m}$ thick protective layer over the active AgBr emulsion. Intrnsic detection efficiency is high and energy independent in the tested range. **Right:** positron beam spot (2D histogram) recorded in a test run of the Talbot-Lau setup, digitized at the Bern microscope scanning facility. The inset shows an example of the raw output from the scanning optical microscope.

Alignment challenges and development of a test electron beam

A Talbot-Lau interferometer produces high contrast interference fringes even with incoherent (i.e. wide and/or poorly collimated) beams. However, the alignment requirements become very strict as coherence decreases (see for example Fig. 6). In our current positron setup we face two main challenges:

- **Rotational alignment of the gratings**: the slits should be parallel within a tolerance $\sigma_\phi \approx 150\,\mu\mathrm{rad}$. One of the gratings sits on a fully non magnetic piezoelectric rotation stage, and a laser alignment procedure can be performed.
- **Positioning of the detector plane**: experimental error on the ratio d_2/d_1 propagates to an uncertainty on the expected location of the interference fringes on the y-axis (the η parameter), at the level of a few mm.

Although a moving (or tilted) emulsion detector can be used to perform a scan on the sensitive parameters, **real time detection** is helpful.

An **electron beam** is being developed at the **Plasma physics laboratory in Milan** to serve as a test bed for real time detectors with a more coherent and intense ($\approx 1 \times 10^9\,\mathrm{s}^{-1}$) beam, and to study in detail the influence of beam coherence on interferometric visibility.

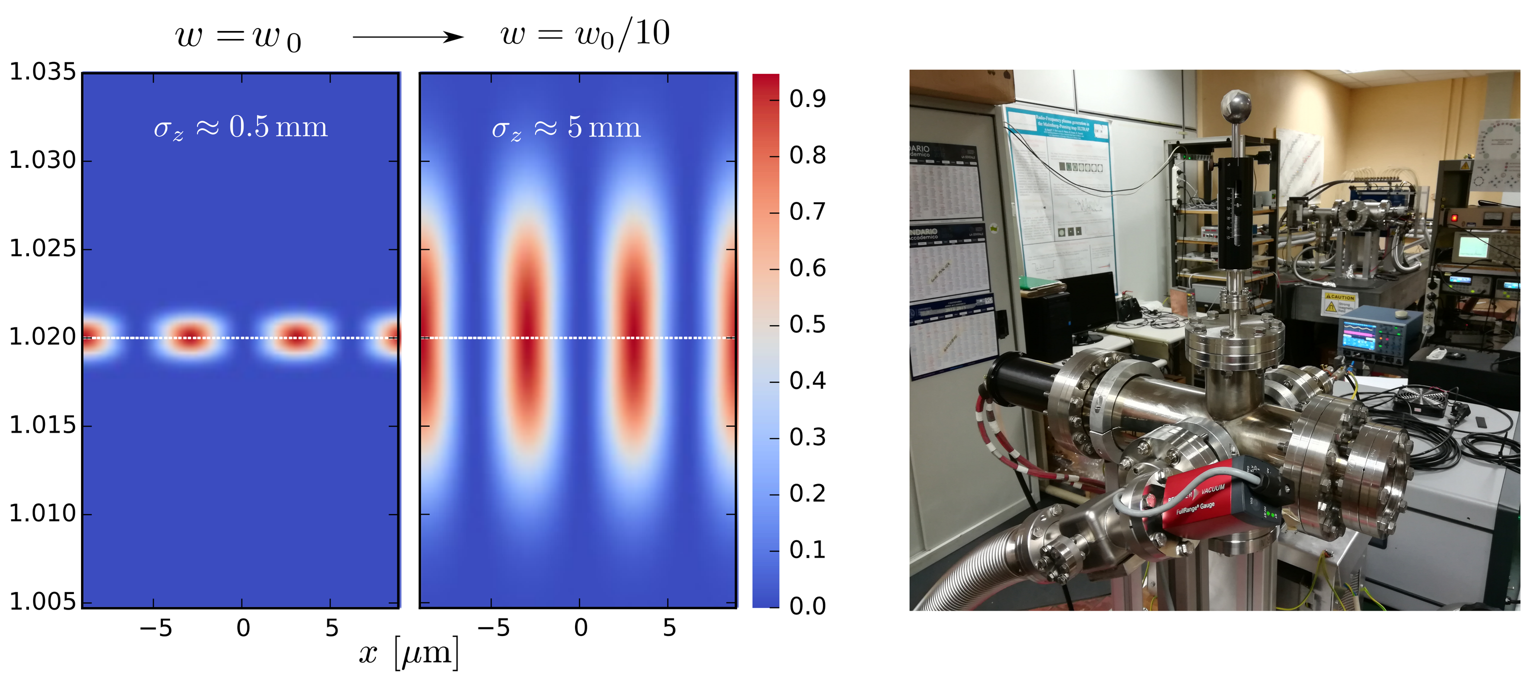

Figure 6: Left: evolution along the optical axis (as an heatmap) of the intensity signal, using a realistic model for the e^+ beam. Sections taken along the y-axis are the interference fringes to be detected. Peak contrast is high ($\approx 95\%$) at the optimal observation distance (dotted line), decreasing rapidly over a distance σ_z. Reduction of the beam width w, for example via mechanical collimation, greatly increases σ_z, at the expense of intensity. **Right:** picture of the electron beam setup.

References

(1) S. Sala et al. Matter-wave interferometry: towards antimatter interferometers. *J. Phys. B*, 48:195002, 2015.
(2) S. Sala et al. Asymmetric Talbot-Lau interferometry for inertial sensing. *Phys. Rev. A*, 94:033625, Sep 2016.
(3) http://lness.como.polimi.it/positron.php.
(4) S. Aghion et al. Detection of low energy antimatter with emulsions. *JINST*, 11(06):P06017, 2016.
(5) T. A. Savas et al. Large-area achromatic interferometric lithography for 100nm period gratings and grids. *J. Vac. Sci. Technol., B*, 14(6):4167–4170, 1996.